



H₂O₂-Activated Mitochondrial Phospholipase iPLA₂ γ Prevents Lipotoxic Oxidative Stress in Synergy with UCP2, Amplifies Signaling *via* G-Protein–Coupled Receptor GPR40, and Regulates Insulin Secretion in Pancreatic β -Cells

Jan Ježek, Andrea Dlasková, Jaroslav Zelenka, Martin Jabůrek, and Petr Ježek

Abstract

Aims: Pancreatic β -cell chronic lipotoxicity evolves from acute free fatty acid (FA)–mediated oxidative stress, unprotected by antioxidant mechanisms. Since mitochondrial uncoupling protein-2 (UCP2) plays antioxidant and insulin-regulating roles in pancreatic β -cells, we tested our hypothesis, that UCP2-mediated uncoupling attenuating mitochondrial superoxide production is initiated by FA release due to a direct H₂O₂-induced activation of mitochondrial phospholipase iPLA₂ γ . **Results:** Pro-oxidant *tert*-butylhydroperoxide increased respiration, decreased membrane potential and mitochondrial matrix superoxide release rates of control but not UCP2- or iPLA₂ γ -silenced INS-1E cells. iPLA₂ γ /UCP2-mediated uncoupling was alternatively activated by an H₂O₂ burst, resulting from palmitic acid (PA) β -oxidation, and it was prevented by antioxidants or catalase overexpression. Exclusively, nascent FAs that cleaved off phospholipids by iPLA₂ γ were capable of activating UCP2, indicating that the previously reported direct redox UCP2 activation is actually indirect. Glucose-stimulated insulin release was not affected by UCP2 or iPLA₂ γ silencing, unless pro-oxidant activation had taken place. PA augmented insulin secretion *via* G-protein–coupled receptor 40 (GPR40), stimulated by iPLA₂ γ -cleaved FAs (absent after GPR40 silencing). **Innovation and Conclusion:** The iPLA₂ γ /UCP2 synergy provides a feedback antioxidant mechanism preventing oxidative stress by physiological FA intake in pancreatic β -cells, regulating glucose-, FA-, and redox-stimulated insulin secretion. iPLA₂ γ is regulated by exogenous FA *via* β -oxidation causing H₂O₂ signaling, while FAs are cleaved off phospholipids, subsequently acting as amplifying messengers for GPR40. Hence, iPLA₂ γ acts in eminent physiological redox signaling, the impairment of which results in the lack of antilipotoxic defense and contributes to chronic lipotoxicity. *Antioxid. Redox Signal.* 23, 958–972.

Introduction

A SIGNIFICANT ANTIOXIDANT role in pancreatic β -cells (1, 2, 9, 13, 23, 28, 29, 31, 42, 45, 48, 54) or α -cells (3) is provided by mitochondrial uncoupling protein-2 (UCP2). This was evidenced for UCP2 KO mice of three highly congenic strain backgrounds, all of which exhibit oxidative

stress (decreased ratios of reduced-to-oxidized glutathione in blood or tissues), elevated levels of antioxidant enzymes, and increased nitrotyrosine content in their islets (42). Pancreatic β -cells from UCP2 KO mice showed chronically higher reactive oxygen species (ROS) when compared with wild-type mice (29). Mice with selective knockout of UCP2 in pancreatic β -cells exhibited increased glucose-induced inner

Department of Membrane Transport Biophysics, Institute of Physiology, Academy of Sciences of the Czech Republic, Prague, Czech Republic.

© Jan Ježek *et al.* 2015; Published by Mary Ann Liebert, Inc. This Open Access article is distributed under the terms of the Creative Commons Attribution Noncommercial License (<http://creativecommons.org/licenses/by-nc/4.0/>) which permits any noncommercial use, distribution, and reproduction in any medium, provided the original author(s) and the source are credited.

Innovation

Fatty acid (FA)-stimulated and redox-stimulated insulin releases have not been fully understood as well as acute lipotoxicity, instantly decreasing insulin secretion in pancreatic β -cells. We describe a feedback antioxidant mechanism based on redox signaling initiated by FA β -oxidation, and promoted plus amplified by mitochondrial phospholipase iPLA₂γ. Not only the antioxidant synergy of iPLA₂γ with mitochondrial UCP2 is demonstrated, but also the iPLA₂γ role in the amplifying mechanism, since further free FAs cleaved by iPLA₂γ serve as “messengers” for G-protein-coupled receptor 40 (GPR40). Consequently, the iPLA₂γ/UCP2 synergy regulates glucose-stimulated, redox-, and FA-stimulated insulin release in pancreatic β -cells.

mitochondrial membrane (IMM) potential ($\Delta\Psi_m$) and elevated intracellular ROS (48).

Superoxide formation is an inevitable side reaction at Complex I and III of mitochondrial respiratory chain (24) and in 2-oxoacid dehydrogenases (41, 46). Mitochondrial superoxide formation increases with an increasing substrate (NADH) load, represented by increasing glucose in pancreatic β -cells (10). Similarly, in numerous situations of local or global electron transfer retardation within the respiratory chain, superoxide production is specifically elevated. This serves for redox signaling, for example, during initiation of hypoxic gene expression remodeling (27).

Mitochondrial H⁺ pumping is usually tightly coupled to the H⁺ backflow *via* the ATP synthase. Since any uncoupling of this accelerates electron transfer within the respiratory chain (and hence respiration), the superoxide formation is attenuated by mitochondrial uncoupling. This represents the key mechanism exerted by UCP2, although it slightly attenuates ATP synthesis. In pancreatic β -cells, the increase in oxidative phosphorylation (OXPHOS) substantiates the canonical mechanism of glucose sensing. The increasing ATP/ADP ratio at higher glucose initiates the glucose-stimulated insulin secretion (GSIS) (5, 26, 47).

By shifting ROS homeostasis, UCP2 may participate in redox signaling in β -cells (31, 48), which may be easily transmitted due to the low capacity of redox buffers (23). H₂O₂-responsive gene expression is manifested for both major differentiation factors of β -cells, PDX-1 and MafA (47). Impaired antioxidant defense leading to chronic oxidative stress may affect insulin secretion machinery that is finely tuned for optimum GSIS in β -cells, as recognized in type 2 diabetes patients (16, 39, 40) and rodent diabetic models (30, 33). ROS may further accelerate diabetic development by promoting apoptosis, thus decreasing β -cell mass (51). Consequently, oxidative stress serves as a mediator of β -cell remission.

The function of UCP1 (12) and recombinant UCP2 (6, 7, 20, 53) is essentially dependent on its anionic transport substrates, nonesterified fatty acids (FAs) (6, 7, 18, 20, 53). However, FAs augment GSIS in β -cells, when exposed for hours (8, 15, 19), but chronically excessive saturated FAs suppress insulin secretion (32, 43, 52), the phenomenon termed lipotoxicity (15, 19). As a simplifying scheme, UCP2 might counteract acute lipotoxicity arising from oxidative stress due to the incoming FAs. Nevertheless, its role should be further clarified.

The role of phospholipases A₂ (PLA₂) (21, 22, 25, 34, 35, 38) residing in (such as iPLA₂β) (34) or recruited to mitochondria of pancreatic β -cells should also be explained in relation to their activation. PLA₂ may amplify lipotoxicity, but in concert with UCP2 a hypothetical synergic antioxidant activity may prevail, such as with mitochondrial iPLA₂γ in heart (25) and lung tissues (21). Both iPLA₂γ and iPLA₂β belong to the group VI of PLA₂s (38) ascribed to the cytosolic Ca²⁺-independent iPLA₂s. They are also termed patatin-like phospholipase domain-containing lipases (PNPLAs), which, besides the release of unsaturated FAs by cleaving the *sn*-2 ester bond of membrane phospholipids, also cleave saturated FAs at the *sn*-1 ester bond (21, 38). The β -isoform is sensitive to a stereo-selective inhibitor *s*-bromo-enol lactone (*s*-BEL), whereas the γ -isoform (PNPLA8) is sensitive to *r*-BEL (22). Alternative splice isoforms of iPLA₂γ 88-, 77-, 74-, and 63-kDa potentially exist, with the 63-kDa being peroxisomal (35).

The FAs were also implicated in the insulin release in pancreatic β -cells. Although the mechanism is not decisively elucidated (15), the G-protein-coupled receptor 40 (GPR40) has been recently implicated in insulin-stimulating responses (11). In addition, the threshold FA concentration, above which acute lipotoxicity is exerted and below which insulin release is stimulated, is not known.

In this work, we aimed at studying how UCP2-mediated antioxidant action may be initiated and regulated and at elucidating its functional relationship with PLA₂s. We revealed the antioxidant synergy of UCP and iPLA₂γ and describe in detail its impact on acute lipotoxicity and insulin secretion in model pancreatic β -cells, insulinoma INS-1E cells.

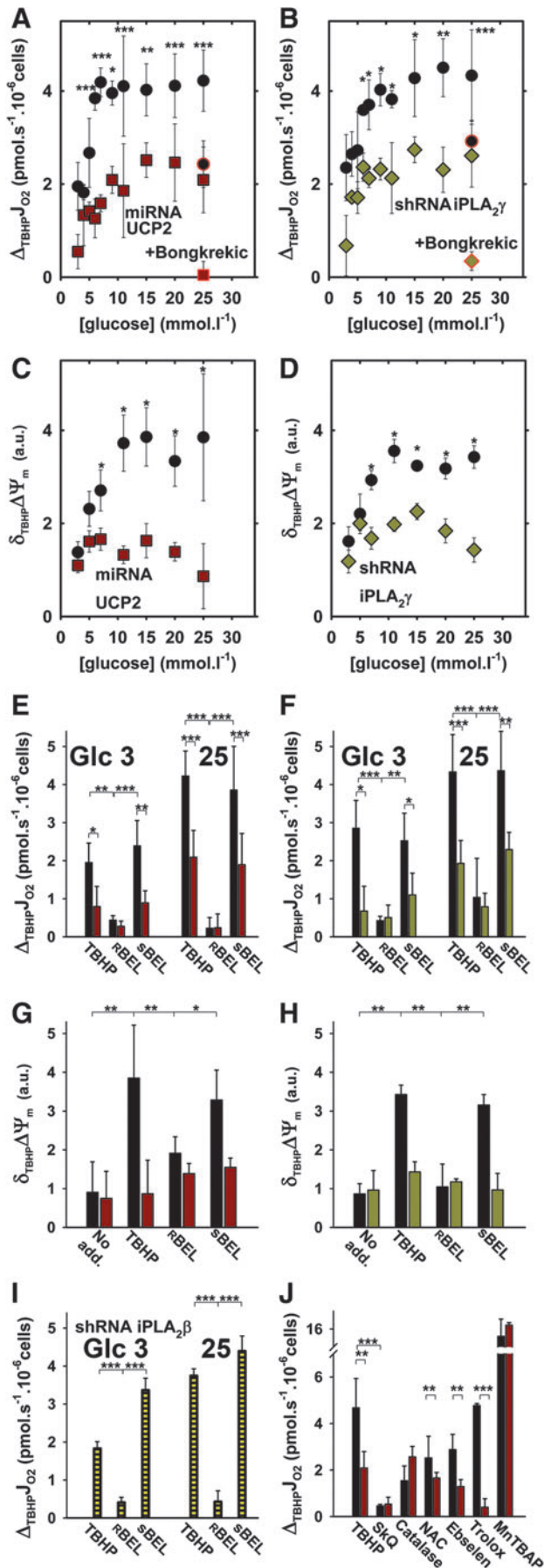
Results

Uncoupling manifested by respiration increase after tert-butylhydroperoxide addition to INS-1E cells is absent in cells silenced for UCP2 or iPLA₂γ

Nontransfected INS-1E cells with glucose lowered to 3 mM still exhibited a substantial respiration of $23.6 \pm 6.3 \text{ pmol O}_2 \cdot \text{s}^{-1} \times 10^{-6} \text{ cells}$ ($n=49$; number of preparations $N=10$). The corresponding state may be regarded as the phosphorylating state-3, although with low substrate levels available for OXPHOS. *Tert*-butylhydroperoxide (TBHP) addition resulted in the acceleration of respiration, so that the differences ($\Delta_{\text{TBHP}}J_{\text{O}_2}$) between respiration rates before ($J_{\text{O}_2}^0$) and after TBHP exhibited a saturating dependence on glucose.

INS-1E cells transfected with nontargeting microRNA (miRNA) (ntgINS-1E cells) and with glucose lowered to 3 mM exhibited virtually unchanged respiration of $J_{\text{O}_2}^0 = 25.3 \pm 6.3 \text{ pmol O}_2 \cdot \text{s}^{-1} \times 10^{-6} \text{ cells}$ ($n=356$; $N=51$) and responded to TBHP in the same way (Fig. 1A). UCP2-silenced cells (Supplementary Fig. S1A, C; Supplementary Data are available online at www.liebertpub.com/ars) with glucose lowered to 3 mM did not change respiration ($J_{\text{O}_2}^0 = 24.2 \pm 7.4 \text{ pmol O}_2 \cdot \text{s}^{-1} \times 10^{-6} \text{ cells}$; $n=358$; $N=58$). However, they responded much less to TBHP addition with increasing glucose (Fig. 1A). The residual response predominantly reflects contribution of the ADP/ATP carrier (25), since it was prevented by bongkreikic acid, which blocked the whole response in UCP2-silenced cells (Fig. 1A).

In addition, iPLA₂γ-silenced cells (Supplementary Fig. S1B, C) with glucose lowered to 3 mM did not significantly



change respiration ($J_{\text{O}_2}^0 = 19.4 \pm 3.9$ pmol $\text{O}_2 \cdot \text{s}^{-1} \times 10^{-6}$ cells; $n = 116$; $N = 23$; compared with own ntg shRNA controls having $J_{\text{O}_2}^0 = 22.4 \pm 3.3$ pmol $\text{O}_2 \cdot \text{s}^{-1} \times 10^{-6}$ cells; $n = 117$; $N = 24$). They also exhibited suppressed respiratory responses to TBHP addition with increasing glucose and complete inhibition by bongkreikic acid (Fig. 1B).

To verify that the observed respiratory elevations represent a mild mitochondrial uncoupling, we monitored the IMM potential decrease ($\delta_{\text{TBHP}}\Delta\Psi_m$) at various glucose concentrations, after TBHP addition to UCP2- (Fig. 1C) and iPLA₂ γ -silenced INS-1E cells (Fig. 1D). We found the same pattern as for respiration increases. Since the accelerated respiration, together with simultaneous $\Delta\Psi_m$ decline, strictly defines mitochondrial uncoupling, we conclude that TBHP induces uncoupling in INS-1E cells in a UCP2- and iPLA₂ γ -dependent manner.

The iPLA₂ γ contribution also stems from the sensitivity to its stereo-selective inhibitor R-BEL, which prevented both TBHP-induced J_{O_2} elevations (Fig. 1E, F and Supplementary

FIG. 1. Tert-butylhydroperoxide (TBHP)-induced respiratory elevation and IMM potential decrease in INS-1E cells. ntgINS-1E cells: black circles or bars; UCP2-silenced cells: dark red squares or bars; iPLA₂ γ -silenced cells: green diamonds or bars; iPLA₂ β -silenced cells: yellow bars (I). ANOVA * $p < 0.05$; ** $p < 0.01$; *** $p < 0.001$. (A, B) Glucose-dependent respiration elevations: Glucose addition to INS-1E cells respiring at state-3 was performed after cell preincubation in a culture medium with 3 mM glucose for 16 h. Subsequently, 250 μM TBHP was added to cells assayed in this medium. The resulting respiration elevation responses $\Delta_{\text{TBHP}}J_{\text{O}_2}$ are plotted versus final glucose concentration ($n = 3-7$ estimations for each concentration, 8-12 for 25 mM glucose). Red-edge symbols: 100 μM bongkreikic acid was present during the assay. (C, D) Glucose-dependent $\Delta\Psi_m$ decrease: TBHP-induced decreases in $\Delta\Psi_m$, $\delta_{\text{TBHP}}\Delta\Psi_m$, were assayed as TMRE fluorescence increase ($F_{\text{TBHP}} - F_0$)/ F_0 between the initial (F_0) and fluorescence after TBHP addition (F_{TBHP}) in relative units ($n = 3$). Uncoupling of mitochondria by 2.5 μM FCCP prevented $\delta_{\text{TBHP}}\Delta\Psi_m$ decreases, which then reached values < 1 (data not shown). This also confirms that plasma membrane potential did not affect the assay. (E-I) R-BEL versus s-BEL inhibition of TBHP-induced uncoupling assayed as respiration elevations $\Delta_{\text{TBHP}}J_{\text{O}_2}$ (E, F, I) or $\Delta\Psi_m$ decreases (G, H). The effects of 40 μM R-BEL ("RBEL") and 40 μM s-BEL ("sBEL") were quantified for cells remaining at 3 mM glucose ("Glc 3" in E, F, I) and cells subjected to 25 mM glucose ("25" in E, F, I) ($n = 3, 11$ for ntg controls and UCP2-silenced cells). (J) Effect of antioxidants on TBHP-induced uncoupling of INS-1E cell respiration: The assay with 25 mM glucose was conducted as in (A) and with antioxidants: 0.5 μM SkQ1 ("SkQ"); 2 mM N-acetyl-L-cysteine ("NAC"); 7.5 μM ebselen; 200 μM Trolox; and 100 μM MnTBAP. "Catalase" represents catalase overexpression. It should be noted that MnTBAP in the presence of TBHP increased oxygen consumption even in the absence of cells, indicating that the observed effects of MnTBAP are not caused by interacting with cells or mitochondria, but by the formation of butylperoxy radicals, initiating peroxidation of the porphyrin organic groups at the expense of oxygen. ANOVA, analysis of variance; FCCP, trifluoromethoxy carbonylcyanide phenylhydrazine; IMM, inner mitochondrial membrane; MnTBAP, Mn(III)tetrakis(4-benzoic acid)porphyrin; s-BEL, s-bromo-enol lactone; TMRE, tetramethylrhodamine ethyl ester; UCP2, uncoupling protein-2.

Fig. S2A) and $\Delta\Psi_m$ drops (Fig. 1G, H), whereas both were unaffected by s-BEL (Fig. 1E–H). In contrast, cells silenced for iPLA₂β responded to TBHP normally and this was not inhibited by s-BEL, the stereo-selective inhibitor of iPLA₂β (Fig. 1I). Similar UCP2- (Supplementary Fig. S2B) and iPLA₂γ-dependent uncoupling (not shown) was induced by TBHP at state-4 set by oligomycin. We have also confirmed that the state-3 respiration of mitochondria isolated from INS-1E cells can be uncoupled in a UCP2-dependent manner (Supplementary Fig. S3).

TBHP-induced uncoupling is prevented by antioxidants

As expected, UCP2-dependent TBHP-induced mitochondrial uncoupling in ntgINS-1E cells at 25 mM glucose was completely prevented by matrix-targeted antioxidant SkQ1 and substantially blocked by catalase overexpression (Fig. 1J). Among nonmitochondrial antioxidants, only *N*-acetyl-L-cysteine and ebselen exhibited moderate prevention. Trolox, an alkyl-peroxyl free radical scavenger, had no effect (Fig. 1J), excluding involvement of lipoperoxidation. A superoxide dismutase (SOD) mimetic, Mn(III)tetrakis(4-benzoic acid)porphyrin (MnTBAP), by direct interaction with TBHP, accelerated TBHP-induced respiration independently of UCP2 presence (Fig. 1J).

iPLA₂γ is directly activated by TBHP or H₂O₂

Reconstituted recombinant iPLA₂γ was reversibly activated by H₂O₂ (Fig. 2A–E) with a half-maximum activation constant AC₅₀ corresponding to ~1.5 nmol H₂O₂ per nmol of enzyme (Fig. 2E). The H₂O₂-induced FA release in proteoliposomes containing iPLA₂γ was fully reversed by membrane-permeable dithiothreitol (DTT) and partially by membrane-impermeable glutathione (Fig. 2D, E). These results indicate that iPLA₂γ activation by H₂O₂ is dependent on reversible oxidation of accessible cysteine residues. In cells, AC₅₀ was 200 μM for TBHP (Supplementary Fig. S2A).

Gas chromatography/mass spectrometry quantification of released FAs from iPLA₂γ-containing proteoliposomes after 60 min at 30°C had indicated a release of approximately 1 nmol⁻¹·min·(mg protein)⁻¹ (1.5% of phospholipid FAs) of free palmitic acid (PA), oleic, or linoleic acid, which was enhanced by H₂O₂, but not with r-BEL (Fig. 2C). GC/MS analysis of TBHP- or PA-induced (*vide infra*) FA release in ntgINS-1E cells 2 min after the addition of 25 mM glucose is summarized in Figure 2F and G. A substantial increase in free FAs occurred only on iPLA₂γ activation by 250 μM TBHP or 75 nmol PA·10⁻⁶ cells, corresponding to 0.2 pmol free PA (other FAs increased, Fig. 2G) and was blocked by 40 μM r-BEL (Fig. 2F, G). Along with unsaturated FAs, palmitic (Fig. 2F) and stearic acid (Fig. 2F, G) also were cleaved, which is characteristic of PNPLA subfamily of phospholipases (38). Consequently, we can conclude that H₂O₂- (*ex vivo* TBHP-) activated or PA-induced (*vide infra*) iPLA₂γ cleaves FAs off mitochondrial phospholipids and provides them to UCP2 as the transport substrates, ensuring slight uncoupling of mitochondria.

Decrease of superoxide release into mitochondrial matrix on TBHP addition is absent in INS-1E cells silenced for UCP2 or iPLA₂γ

We further investigated whether the observed TBHP-induced uncoupling attenuates mitochondrial superoxide

production. We employed MitoSOX Red fluorescence (10), measuring the *in situ* surplus superoxide release into the mitochondrial matrix as the rate J_m of fluorescence changes in regions of interests identical to the matrix (Supplementary Movie S1). We have evaluated (Fig. 3A, D) how J_m is altered after the immediate TBHP addition to ntgINS-1E cells pre-equilibrated with 25 mM glucose for 10 min (after 16-h preincubation with 3 mM glucose). In spite of the pro-oxidant nature of TBHP, J_m rates decreased to a minimum on TBHP addition (Fig. 3A, D). Such attenuation of mitochondrial superoxide production ceased in the presence of r-BEL, but not s-BEL (Fig. 3A, D), and was not observed in UCP2- (Fig. 3B, C) and iPLA₂γ-silenced INS-1E cells (Fig. 3E, F).

We conclude that iPLA₂γ and UCP2 synergy provides a suppression of mitochondrial superoxide production by mild uncoupling initiated by the TBHP-mediated activation of iPLA₂γ. Consequently, we predict that in pancreatic β-cells the H₂O₂-activated iPLA₂γ/UCP2 synergy provides an antioxidant mechanism, enabling a feedback downregulation of oxidative stress.

iPLA₂γ activation during β-oxidation of palmitate in INS-1E cells

Mitochondrial iPLA₂γ was also activated in ntgINS-1E cells by a matrix ROS/H₂O₂ burst, resulting from the ongoing β-oxidation of the added PA (Fig. 2E). The electron-transfer flavoprotein:ubiquinone oxidoreductase forms superoxide during β-oxidation (41, 46, 50). Superoxide can be instantly transformed to H₂O₂ by SODs. We hypothesized that the resulting H₂O₂ directly activates iPLA₂γ. Our results with the reconstituted recombinant iPLA₂γ (Fig. 2A–C) and experiments described next confirmed this hypothesis. Thus, PA addition induced respiratory elevation (Fig. 4A, B) and $\Delta\Psi_m$ decrease (Fig. 4C, D), indicating mild mitochondrial uncoupling. Respiratory elevations, due to PA ($\Delta P_A J_{O_2}$), were more than two times higher in 25 mM glucose than in 3 mM glucose, and occurred even in the presence of s-BEL but not r-BEL (Fig. 4A, B), indicating the iPLA₂γ specificity. Importantly, the PA-induced uncoupling was virtually absent in cells silenced for either UCP2 (Fig. 4A, C) or iPLA₂γ (Fig. 4B, D).

Altogether, these data suggest that FAs instantly cleaved off phospholipids by iPLA₂γ to determine the UCP2-mediated uncoupling, and that UCP2 requires such a specific nascent FA delivery (for UCP1 see Ref. 11). This is because no response to PA addition took place in the presence of r-BEL (but not s-BEL) in ntgINS-1E cells. Analogously, a negligible response was also observed in iPLA₂γ-silenced cells where UCP2 had to be intact. We have also demonstrated that PA can be substituted by palmitoyl-DL-carnitine administered to cells by Lipofectamine 2000 (Fig. 4E) but not by DL-α-glycerolphosphate (Fig. 4F). Both the β-oxidation inhibitor etomoxir and r-BEL inhibited palmitoyl-DL-carnitine-induced respiratory rise (Fig. 4E). The DL-α-glycerolphosphate-driven respiration was higher in UCP2-silenced cells and was inhibited by a membrane-permeable succinate analog dimethylsuccinate (Fig. 4F) but not by r-BEL (not shown).

A similar antioxidant effect in the mitochondrial matrix (Fig. 3G, H) as seen with TBHP activation of iPLA₂γ was found for iPLA₂γ activation by H₂O₂, resulting from the pro-oxidant PA β-oxidation (Fig. 5C). The superoxide release (J_m) rates declined to a minimum on the PA addition

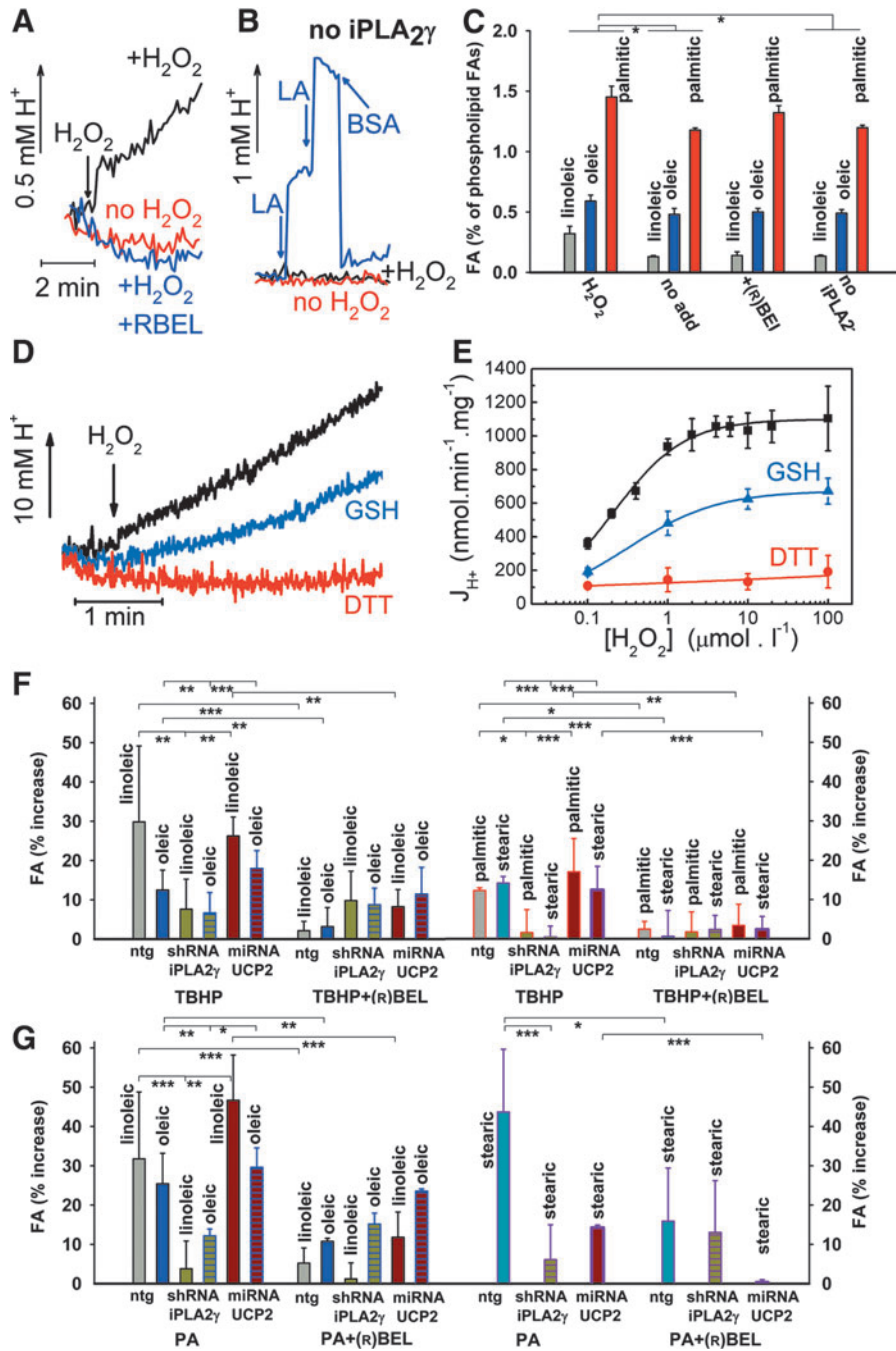


FIG. 2. Redox-dependent free FA release in proteoliposomes with recombinant iPLA₂γ (A–E) and in INS-1E cells (F, G). (A, B, D, E) Fluorimetrically indicated free FA release: Passive diffusion (flip) of FAs into the liposome interior was monitored by sulfopropylquinolinium fluorescence, which increases due to intraliposomal acidification concomitant to FA release. The fluorescence increase was induced by 25 μM H₂O₂ (“+H₂O₂”) in (A, C, D) and was absent without H₂O₂ (“no H₂O₂”) in (A). Inhibition by 1 μM R-BEL (“+H₂O₂+R-BEL” in A), 10 mM glutathione (“GSH” in D, E), or 10 mM dithiothreitol (“DTT” in D, E) is also shown. (B) Without iPLA₂γ (“no iPLA₂γ”), H₂O₂ caused no intraliposomal acidification (“+H₂O₂”) and the response was identical to the baseline (“no H₂O₂”) in contrast to two additions of 10 μM linoleic acid (“LA”), causing the instant intraliposomal acidification. Five micromolar bovine serum albumin (“BSA”), removing FAs, led to subsequent alkalization back toward the initial pH values. Proteoliposomes contained 0.04 μg of purchased (A, C) or 0.4 μg of the affinity-purified (D, E) recombinant human iPLA₂γ per mg of phospholipids. (E) The H₂O₂ dose response for redox-stimulated FA-induced acidification rate is shown, yielding AC₅₀ of 0.2 μM H₂O₂, corresponding to 1.4 nmol H₂O₂ per nmol iPLA₂γ. (C, F, G) GC/MS quantification of free FAs cleaved during 60 min at 30°C as induced by 25 μM H₂O₂ (“H₂O₂”) in iPLA₂γ–proteoliposomes (C) with 0.04 μg of the purchased protein (Novus); or free FAs cleaved during 2 min at 37°C in INS-1E cells, ntg or silenced as ascribed (F, G), supplied with 25 mM glucose, as induced by 250 μM TBHP (F) or 75 nmol PA · 10⁻⁶ cells, corresponding to 0.2 pmol free PA (G). Indicated FAs were detected in the absence of H₂O₂ or TBHP (“no add.”), the presence of 25 μM H₂O₂ (“H₂O₂”), 250 μM TBHP (“TBHP”), or 150 μM PA with 5% BSA; or additional 1 μM (C) or 40 μM (F, G) R-BEL (“+R-BEL”). Averages ± s.d. of 3–7 (G) or 4–17 estimations are shown, recalculated relatively to the estimated total content of FA side chains (C) or the initial FA content (F, G). ANOVA: **p* < 0.1; ***p* < 0.05; ****p* < 0.001. FA, fatty acid; GC/MS, gas chromatography/mass spectrometry; PA, palmitic acid.

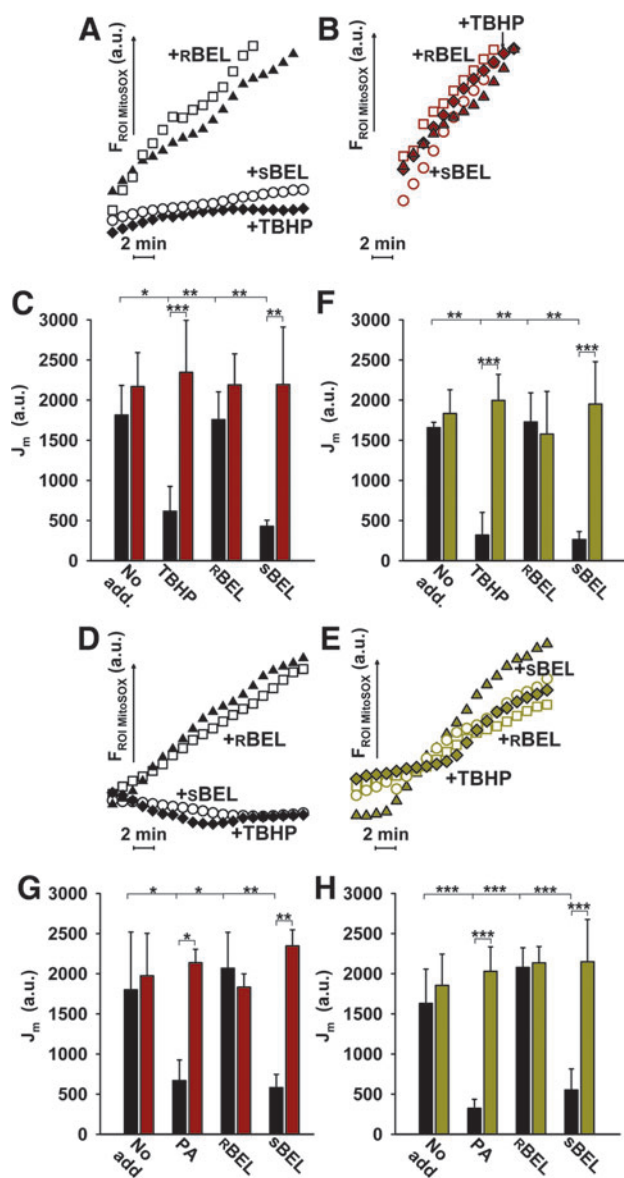


FIG. 3. Prevention of matrix-released superoxide after TBHP (A–F) or PA (G, H) addition is absent in UCP2- or $iPLA_2\gamma$ -silenced cells. ntgINS-E cells of the corresponding scrambled sequences: *black symbols or bars*; UCP2-silenced cells: *dark red symbols or bars*; $iPLA_2\gamma$ -silenced cells: *green symbols or bars*. ANOVA ($n=3-6$): * $p < 0.05$; ** $p < 0.01$; *** $p < 0.001$. Rates of superoxide release into the mitochondrial matrix were assayed by confocal microscopy using MitoSOX Red. The magnitude of J_m in arbitrary units (a.u.) was determined as a slope of linearized fluorescence intensity traces *versus* time (exemplified in **A, B, D, E**). Cells were preincubated with 3 mM glucose for 16 h and glucose was raised to 25 mM at the beginning, while the assay was conducted with no other agent (*triangles*) or as indicated with 25 μ M TBHP (*diamonds*), or with TBHP plus 5 μ M R-BEL (*squares*, “+RBEL”), or with TBHP plus 5 μ M s-BEL (*circles*, “+sBEL”). (**C, F**) Quantifications of J_m rates: The effects of R-BEL were quantified for J_m after TBHP induction of mitochondrial uncoupling (“TBHP”) or without TBHP (“No add.”). (**G, H**) Quantifications of J_m rates during β -oxidation of palmitate in INS-1E cells: The effects of R-BEL were quantified for J_m after PA induction of mitochondrial uncoupling (“PA”; 15 μ M PA) or without PA (“No add.”).

(Fig. 3G, H). Such attenuation of mitochondrial superoxide production ceased in the presence of R-BEL but not s-BEL (Fig. 3G, H), and this was not observed in UCP2- (Fig. 3G) and $iPLA_2\gamma$ -silenced cells (Fig. 3H). We conclude that self-attenuation of oxidative stress at FA β -oxidation exists in INS-1E cells due to the UCP2/ $iPLA_2\gamma$ synergy.

FA-induced uncoupling is prevented by antioxidants

The PA-induced $iPLA_2\gamma$ /UCP2-dependent mitochondrial uncoupling in INS-1E cells at 25 mM glucose was prevented by the matrix-targeted antioxidant SkQ1, by ebselen but not by *N*-acetyl-L-cysteine (Fig. 4G). Unlike with TBHP, it was also blocked by Trolox and MnTBAP (Fig. 4G), reflecting superoxide and down-stream radical formation by β -oxidation. It was also blocked by catalase overexpression (Fig. 4G), which abolished the resulting attenuation of superoxide formation (Fig. 4H).

Concomitant redox changes in the cytosol of INS-1E cells

We have also studied redox changes in the cytosol of ntgINS-1E cells and confirmed that both PA β -oxidation (Fig. 5A–D) and, as expected, TBHP additions (not shown) oxidize cytosol, when rates of oxidation (J_c) were indicated by the cytosolic ROS fluorescent probe CellROX immediately after insults (Fig. 5C, D). However, when detected ~ 15 min after PA addition, the cytosolic oxidation rates J_c were faster in UCP2- (Fig. 5A) and $iPLA_2\gamma$ -silenced cells (Fig. 5B) when compared with ntgINS-1E cells. This difference ceased in the presence of R-BEL. We interpret that after the initial phase of β -oxidation, producing a substantial burst of superoxide converted thereafter to H_2O_2 penetrating to the cytosol (Fig. 5C, D), the resulting $iPLA_2\gamma$ activation and the concomitant UCP2/ $iPLA_2\gamma$ antioxidant synergy later gradually reverses the established pro-oxidant state of the cytosol. The overall ROS release rates to the cytosol are therefore attenuated (Fig. 5A, B).

Mitochondrial $iPLA_2\gamma$ -cleaved free FAs are accessible for plasma membrane

A confocal microscopy assay with the extracellular fluorescent free FA indicator ADIFAB2 demonstrated FA binding to the extracellular ADIFAB2, which ceased in $iPLA_2\gamma$ -silenced cells (Fig. 5E, F). This demonstrates that FAs cleaved by $iPLA_2\gamma$ in mitochondria can be exported to bind to the extracellular ADIFAB2 and therefore are also accessible to the entire cell cytosol and plasma membrane.

Role of UCP2/ $iPLA_2\gamma$ synergy in insulin release

Next, we set to analyze in detail the behavior of the glucose sensor. INS-1E cells with glucose lowered to 3 mM responded to the increasing glucose by elevating the respiration in a saturated manner till the final 25 mM glucose (49). ntgINS-1E cells responded in the same way (Fig. 6A). With the UCP2 silencing, beginning at 9 mM glucose, this relationship was shifted to higher respiration increases (Fig. 6A), indicating that mitochondria lacking UCP2 respond to a higher extent on GSIS. It is known that not only respiration but also $\Delta\Psi_m$ increases after glucose addition (49), and this

was observed in ntgINS-1E cells (Fig. 6C). Again, these $\Delta\Psi_m$ elevations at GSIS were higher in UCP2-silenced cells (Fig. 6C). In contrast, both respiratory (Fig. 6B) and $\Delta\Psi_m$ responses (Fig. 6D) to glucose in iPLA₂ γ -silenced cells were identical to their corresponding ntg controls. We conclude that UCP2 presence in ntgINS-1E cells diminishes respiratory and $\Delta\Psi_m$ responses to the added glucose. These responses are intimately inherent to the glucose-sensing function of pancreatic β -cells. Hence, the UCP2 presence sacrifices a small portion of the glucose-sensing capacity (function range) for benefits of antioxidant protection. The

simplest reasoning predicts that UCP2 does it *via* a mild uncoupling of mitochondria at state-3 (*i.e.*, at phosphorylating state). This is supported by the observed, slightly increased respiration on UCP2 silencing.

However, the rates of glucose-stimulated insulin release in UCP2- or iPLA₂ γ -silenced INS-1E cells were equal to ntgINS-1E controls (Fig. 7A). In the presence of TBHP addition, nonlinear (biphasic) insulin release was initially faster and attained higher magnitudes 10–60 min after glucose addition to UCP2- and iPLA₂ γ -silenced INS-1E cells (Fig. 7B), demonstrating that unchanged and lower-magnitude insulin release rates in ntgINS-1E controls are depressed (45) in the presence of a pro-oxidant due to the iPLA₂ γ /UCP2-initiated uncoupling, similarly as previously observed (48). Hence, a portion of maximum possible insulin-secreting capacity is sacrificed for benefits of antioxidant protection. But independently of TBHP presence, ATP cell levels were equal 60 min after glucose addition, to all studied cells, to ntgINS-1E, UCP2- (Fig. 6E) and iPLA₂ γ -silenced cells (Fig. 6F). This implies that mild uncoupling is not able to substantially block OXPHOS, hence ATP synthesis in the long term. It should be noted, however, that TBHP alone accelerated insulin release in the absence of glucose, causing the redox-stimulated insulin secretion (RSIS) (*cf.* dashed fits in Fig. 7B vs. 7A).

Similar to TBHP, but to a much higher extent, externally added PA extremely elevated insulin release (also together with H₂O₂/ROS generated during its pro-oxidant β -oxidation). PA induced higher rates of insulin release and its nonlinear time course even in the absence of glucose in ntgINS-1E cells (Fig. 7Ca, black dashed fit). This was not altered in cells with

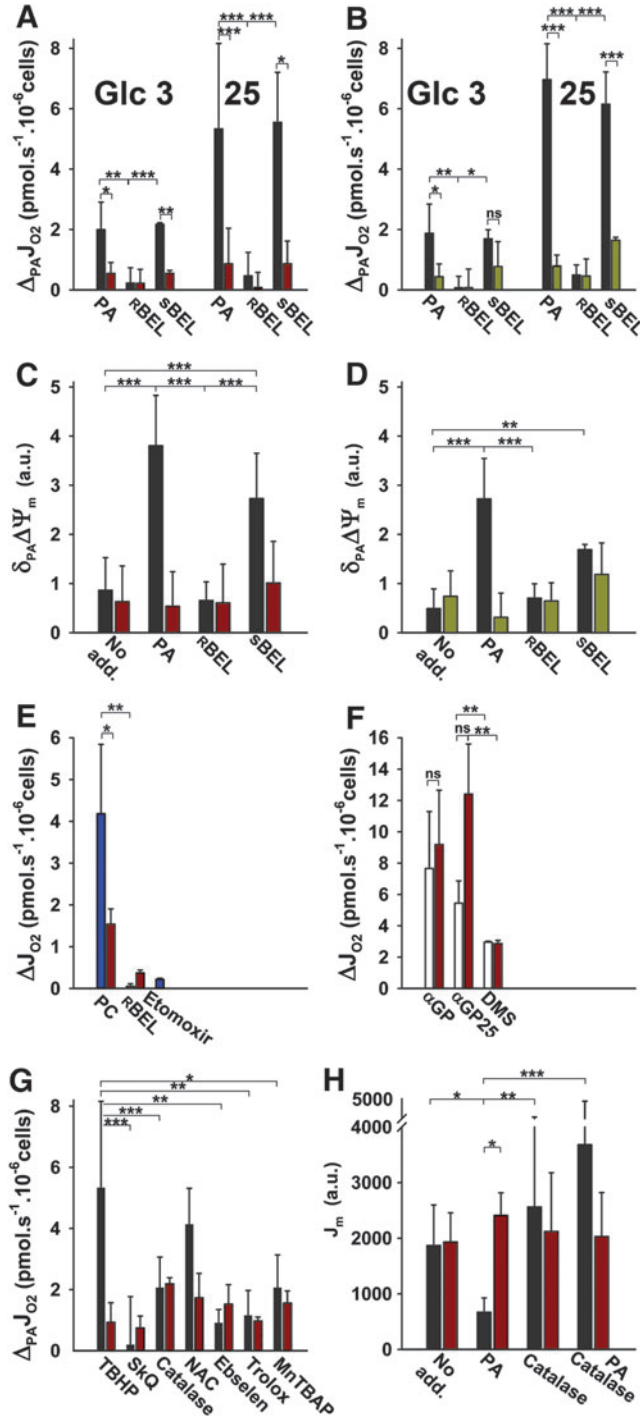


FIG. 4. iPLA₂ γ activation during β -oxidation of palmitate in INS-1E cells. Color coding as in Figure 3. The effects of r-BEL and s-BEL were quantified for PA-induced acceleration of cell respiration, differences ($\Delta_{PA}J_{O_2}$) in respiration before and after the addition of 75 nmol PA·10⁻⁶ cells (**A, B**) in the presence of 3 mM glucose (“Glc 3”) and 25 mM glucose (“25”), and decreases (δ_{PA}) in IMM potential $\Delta\Psi_m$ in the presence of 25 mM glucose (**C, D**). The $\Delta\Psi_m$ decrease was assayed as a TMRE fluorescence increase ($F_{PA}-F_0$)/ F_0 from the initial (F_0) to the elevated fluorescence after PA (F_{PA}) in relative units. Uncoupling of mitochondria by 2.5 μ M FCCP prevented $\delta_{PA}\Delta\Psi_m$ decreases, which then reached values <0.5 (data not shown). Both r-BEL and s-BEL were 40 μ M. ANOVA ($n=3-12$): * p <0.05; ** p <0.01; *** p <0.001. (**E, F**) The effects of palmitoyl-DL-carnitine (**E**) or DL- α -glycerolphosphate (**F**). The effects are shown (**E**) for 40 μ M r-BEL or 50 μ M etomoxir on respiratory responses to additions of 100 μ M palmitoyl-DL-carnitine administered with 2 μ l of Lipofectamine 2000 (at 3 mM glucose); (**F**) for 11 mM dimethylsuccinate (“DMS”) on respiratory responses to additions of 5 mM DL- α -glycerolphosphate at 3 mM glucose (“ α GP”) or 25 mM glucose (“ α GP25”). ANOVA ($n=3-12$): * p <0.05; ** p <0.01; ns, nonsignificant differences. (**G, H**) The effects of antioxidants on β -oxidation of palmitate in INS-1E cells: respiration assays at 25 mM glucose such as in panel A (**G**) or MitoSOX J_m assay (**H**) were conducted in the presence of antioxidants as indicated: 0.5 μ M SkQ1; 2 mM N-acetyl-L-cysteine; 7.5 μ M ebselen; 200 μ M Trolox; and 100 μ M MnTBAP. “Catalase” represents catalase over-expression. ANOVA ($n=6$): * p <0.05; ** p <0.01; *** p <0.001.

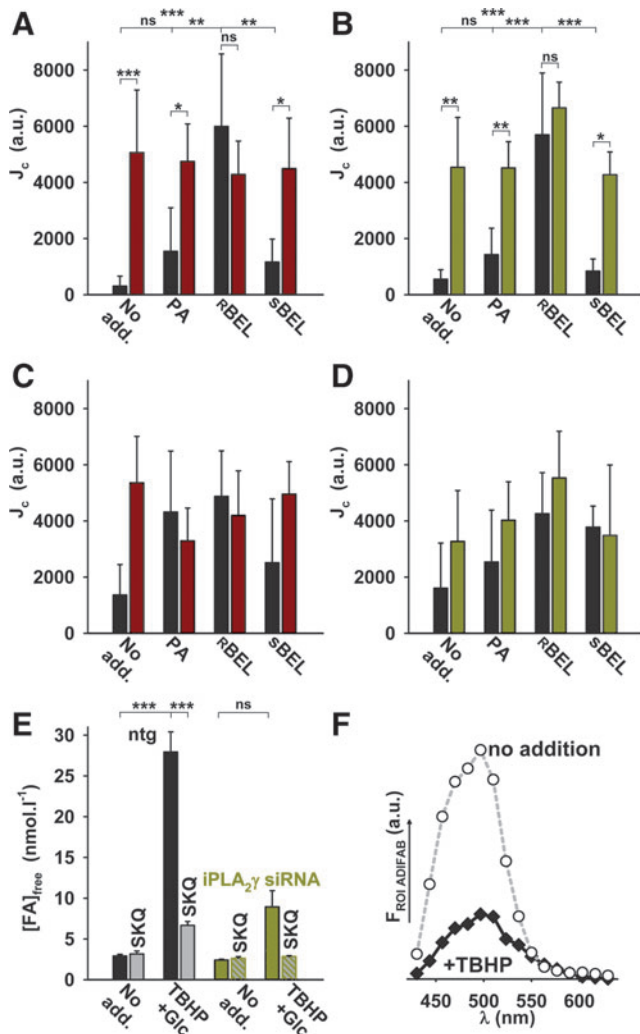


FIG. 5. Cytosolic ROS and extracellular FA monitoring in INS-1E cells. (A–D) Antioxidant effect of UCP2 and iPLA₂γ synergy activated by β -oxidation of palmitate. For color coding, see Figure 3. Rates of cytosolic oxidation J_c (ROS plus oxidized SH residues) were monitored by confocal microscopy using CellROX after additions of 15 μ M PA. The J_c rates were taken after 15 min (A, B) or during the first 5 min (C, D). Both R-BEL and s-BEL were 50 μ M. ANOVA ($n=6-9$): * $p < 0.05$; ** $p < 0.01$; *** $p < 0.001$. (E, F) TBHP-induced free FA release was detected by confocal microscopy in the extracellular space based on quenching of ADIFAB2 fluorescence. Pericellular FA concentration values (E) were estimated from spectra (exemplified in F) obtained in the regions of interest selected around the outer perimeter of GFP-positive cells before and after the addition of glucose to the final 25 mM and 12.5 μ M TBHP, using a dissociation constant of 50 nM, which corresponds to an average value for plasma/serum FAs (cf. ADIFAB2 protocols, FFA Sciences, www.ffasciences.com). Where indicated, 200 nM SkQ1 was present (“SKQ”). GFP, green fluorescent protein; ROS, reactive oxygen species.

silenced phospholipase D (Supplementary Fig. S4). Surprisingly, in UCP2- and iPLA₂γ-silenced INS-1E cells, PA promoted much less of the glucose-insensitive insulin release, regarding to an extent and also rates, for iPLA₂γ-silenced cells (Fig. 7Cb, Cc, dark red dashed or green dashed fit). At 15 μ M

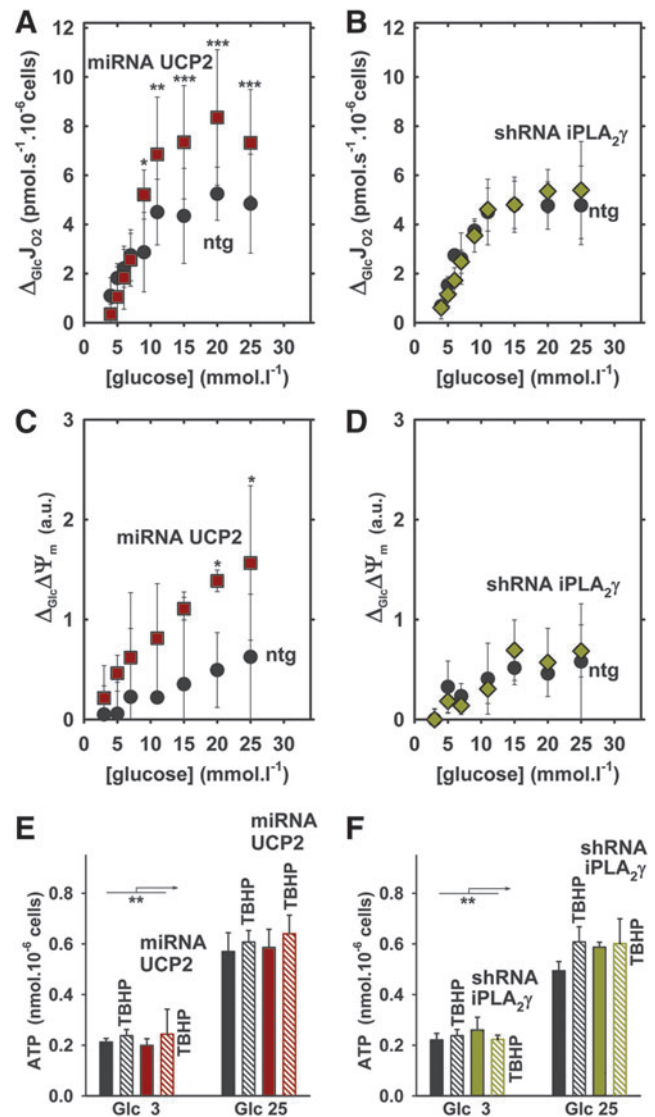


FIG. 6. Changes after glucose addition to control, UCP2- or iPLA₂γ-silenced cells. For color and symbol coding, see Figure 1. Cells were preincubated for 16 h in a cultivation medium with 3 mM glucose and assayed in it. Responses to the additional glucose with its indicated final concentration are shown for: (A, B) Respiratory elevations ($n=9-25$; $n=110$ for 25 mM glucose); ANOVA: * $p < 0.05$; ** $p < 0.01$; *** $p < 0.001$; (C, D) IMM potential increases $\Delta_{Glc} \Delta \Psi_m$ ($n=3$), taken as TMRE fluorescence decreases $(F_0 - F_{Glucose})/F_0$ from the initial (F_0) to the decreased fluorescence after glucose ($F_{Glucose}$) in relative units. Uncoupling of mitochondria by 2.5 μ M FCCP prevented $\delta_{TBHP} \Delta \Psi_m$ increases, which then reached values < 0.1 (data not shown). ANOVA: * $p < 0.05$; (E, F) cytosolic ATP levels in the absence or presence of TBHP (250 μ M; dashed bars) assayed with no further addition (“Glc 3”) or after glucose adjustment to 25 mM (“Glc 25”). ATP levels were quantified after 60 min. ANOVA ($n=4-11$): ** $p < 0.05$.

PA (~ 4 pmol $\times 10^{-6}$ cells), glucose only slightly further increased the already fast insulin release in ntgINS-1E and also the relatively slower insulin release in iPLA₂γ-silenced cells (Fig. 7Cb, Cc dark red or green fit). In UCP2-silenced cells, 15 μ M PA with glucose promoted an insulin release extent,

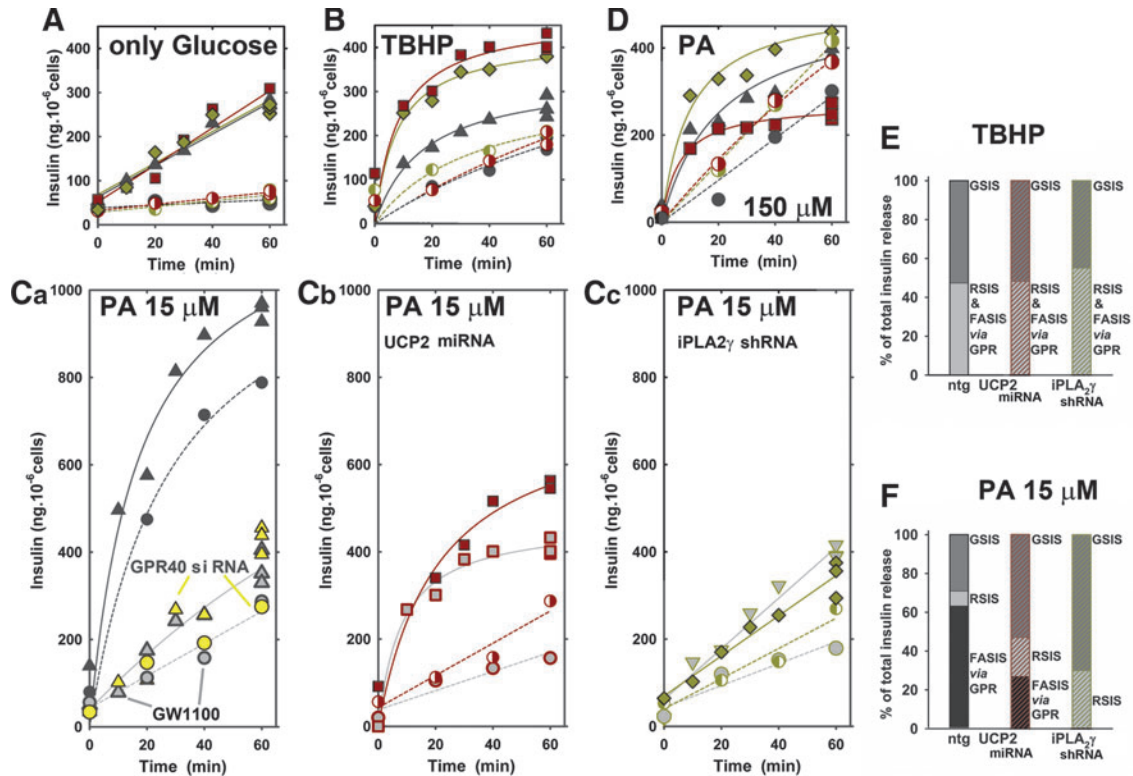


FIG. 7. Glucose-stimulated insulin release in the absence or presence of pro-oxidant insult. Changes in insulin release into Krebs-Ringer HEPES buffer were assayed: (A) in the absence or (B) presence of TBHP (25 μM); or (Ca, Cb, Cc) 15 μM and (D) 150 μM PA, all added together with glucose, during 60 min after raising glucose to 25 mM or without glucose addition (*dashed fits and semi-filled symbols or gray circles or black circles for ntg INS-1E cells*). *Black symbols or fits*: ntg INS-1E cells; *dark red symbols or fits*: UCP2-silenced cells; *green symbols or fits*: iPLA₂ γ -silenced cells. (Ca, Cb, Cc) *Yellow-filled symbols* indicate data of GPR40-silenced cells; the *gray-filled symbols* represent measurements in the presence of GPR40 antagonist GW1100, added at the beginning. (E, F) Typical components extracted from (B) are shown in (E) and of (A, C) in (F), for GPR40-relevant fatty acid-stimulated insulin secretion (FASIS *via* GRPR), redox-stimulated insulin secretion (RSIS) and GSIS. Before the experiment, cells were routinely cultivated with 11 mM glucose, transferred to the Krebs-Ringer HEPES buffer, and incubated in it for 10 min before glucose addition. Rates of insulin release were 3.7 ± 0.2 , 4.2 ± 0.5 , or $3.6 \pm 0.4 \text{ ng} \cdot \text{min}^{-1} \times 10^{-6}$ cells in the absence of TBHP and 6.3 ± 1.5 , 9 ± 3 , or $12 \pm 5 \text{ ng} \cdot \text{min}^{-1} \times 10^{-6}$ cells during first 20 min in the presence of TBHP in ntg controls, UCP2-silenced or iPLA₂ γ -silenced cells, respectively. (C) Rates of insulin release with 15 μM PA were 16 ± 2 , 2.5 ± 0.1 , or $2.4 \pm 0.1 \text{ ng} \cdot \text{min}^{-1} \times 10^{-6}$ cells in the absence of glucose and 22 ± 8 , 12 ± 3 , or $5.3 \pm 0.8 \text{ ng} \cdot \text{min}^{-1} \times 10^{-6}$ cells during first 20 min with glucose in ntg controls, UCP2-silenced or iPLA₂ γ -silenced cells, respectively. GPR40, G-protein-coupled receptor 40; GSIS, glucose-stimulated insulin secretion.

attaining $\sim 50\%$ of levels in ntgINS-1E cells after 60 min. It should be noted that at 15 μM PA, the majority of PA is bound to the albumin present and partitioned into membranes, whereas only $\sim 1.3 \text{ nM}$ PA was free in our experiment, representing a concentration comparable to normal plasma levels. The time course was similar to that with the TBPH pro-oxidant insult (Fig. 7Cb vs. 7B). Similar results were obtained with 30 μM PA (not shown). To simulate acute lipotoxicity, we used a much higher PA (150 μM ; exceeding 200 nM free PA). Here, the net GSIS was reduced down to 25% (Fig. 7D), indicating such an acute lipotoxicity that overcomes the stimulating effect of PA. As a result, the insulin release in the absence of PA was equal to the one with PA in UCP2- and iPLA₂ γ -silenced cells.

Redox-activated iPLA₂ γ supplies FAs for GPR40-stimulated insulin release

Surprisingly, the GPR40, previously indicated to act in insulin-stimulating responses (11), turned out to be a major

player in excessive rates of PA-insulin release in ntgINS-1E cells (Fig. 7Ca). This conclusion stems from the finding that in GPR40-silenced cells (Fig. 7Ca, yellow symbols) and in ntgINS-1E cells subjected to the GPR40 antagonist GW1100 (Fig. 7Ca, gray symbols) the PA-induced insulin release was profoundly inhibited to the levels induced by TBHP (Fig. 7B) in both the absence and presence of glucose. In UCP2-silenced cells, where intermediate PA-induced insulin release rates *versus* ntg controls were assessed, GW1100 also slightly inhibited the PA-induced insulin release (Fig. 7Cb). In contrast, in iPLA₂ γ -silenced INS-1E cells, GW1100 had no effect in the presence of glucose and its effect was very small in the absence of glucose (Fig. 7Cc).

Taken together, we interpret these results as follows: In the situation where, promoted by sole FA β -oxidation, ROS activate insulin release in the absence (the net RSIS; Fig. 7E, F) or presence of glucose (RSIS plus GSIS, Fig. 7E, F), the lack of iPLA₂ γ evidently causes that no further FAs are cleaved, in contrast to the ongoing cleavage in ntg or UCP2-silenced

autocrine and paracrine interrelationships. They evoke certain limitations of our *in vitro* system used.

Rather complex results were obtained for FASIS or FASIS combined with GSIS (Fig. 7Ca, E, F). At low (15 μ M, corresponding to 1.3 nM free) PA, the overall FASIS + GSIS is lower in UCP2- and iPLA₂ γ -silenced cells *versus* ntg cells, in spite of the tighter mitochondrial coupling *versus* ntg cells. The two components are involved in FASIS. The first one stems from the insulin release activated *via* the GPR40 pathway (11) (Fig. 7C). The second one represents the net RSIS and is solely manifested in iPLA₂ γ -silenced cells without glucose. The GPR40 pathway of insulin secretion can be activated and is strongly amplified (Fig. 8B) by FAs cleaved off phospholipids by iPLA₂ γ . Lysophospholipids remaining after the iPLA₂ γ reaction could be hypothetically cleaved by specific mitochondrial phospholipase D (mtPLD) (14), but as demonstrated this does not affect FASIS (Supplementary Fig. S4). FAs are involved in the glycerol lipid/FA cycle signaling stimulating insulin secretion (44).

The iPLA₂ γ is most likely initially activated *in vivo* by the pro-oxidant β -oxidation of FAs incoming from the blood. During FA β -oxidation, activation of iPLA₂ γ by H₂O₂ burst arises from the electron-transfer flavoprotein:ubiquinone oxidoreductase (41, 46, 50) and SODs activities. The situation resembles a self-accelerating cycle, since more active iPLA₂ γ provides more FAs for further β -oxidation, which further elevates ROS/H₂O₂. Besides iPLA₂ γ , these surplus ROS/H₂O₂ themselves trigger insulin secretion and, in parallel, persistently cleaved FAs promote GPR40 activation. All these contributors add on the resulting overstimulation of insulin secretion (Fig. 7Ca), which is permanent (unlike with a single bolus of TBHP) until the added PA is metabolized. In its intermediate state, certain overstimulation is also possible with ablated UCP2 but logically not with ablated iPLA₂ γ . We estimated that at 15 μ M PA plus glucose, the insulin release induced during 60 min consists of ~30% net GSIS, <10% net RSIS, and 60% GPR40 pathway (Fig. 7F). The activation of the GPR40 pathway vanished with ablated iPLA₂ γ . Without UCP2, hence at a more coupled state without antioxidant protection, the net GSIS increases to >50% and RSIS is doubled (Fig. 7F). Similar 50% net GSIS existed with TBHP (Fig. 7E), inducing the net RSIS in the absence of glucose.

We also conclude that UCP2-mediated mild uncoupling is initiated only when free FAs are directly cleaved off the phospholipids at the UCP2 vicinity (7) by iPLA₂ γ (for UCP1 see Ref. 12). In other words, only the nascent FAs are capable of initiating UCP2-mediated uncoupling and a simple PA addition to cells is insufficient (Fig. 4B). FAs are considered the UCP2 cycling/wobbling substrates/cofactors, respectively, essential for their uncoupling function (6, 7, 12, 18, 20, 53).

Demonstrating UCP2/iPLA₂ γ antioxidant synergy and initiation of UCP2-mediated mild uncoupling by a nascent FA, we have resolved some contradictions that have been reported during the past decade for UCP2 role in pancreatic β -cells. Various reports of ROS-activated UCP2 function (1, 28) can be alternatively explained by the ROS-initiated iPLA₂ γ activation providing FAs for UCP2. Previously, a mild uncoupling in mitochondria isolated from INS-1E cells was also linked to UCP2, while accounting for approximately 30% of H⁺ leak (1, 2). Unlike negative demonstrations (13), we now show that UCP2 is activated exclusively by nascent

FAs. This ensures that the net glucose sensing in pancreatic β -cells is not substantially affected by mild uncoupling, unless acute lipotoxicity and/or excessive oxidative stress activate the nascent FA delivery toward UCP2 by iPLA₂ γ . One would predict that the lack of either UCP2 or iPLA₂ γ must result in an easier reach of the oxidative stress threshold from which a pathological outcome is initiated. These characteristics were reported for UCP2 ablation (29, 42, 48).

The unique feature of the iPLA₂ γ protective role is represented by the fact that iPLA₂ γ is not constitutively active. Hence, without redox signaling or excessive oxidative stress (such as resulting in acute lipotoxicity), iPLA₂ γ does not contribute to mitochondrial uncoupling and to the diminished insulin release (Fig. 7A, B). In turn, when activated, its synergy with UCP2 leads to the antioxidant protection at the expense of insulin release. Unless redox activated, no other mitochondria-localized PLA₂ isoform can substitute iPLA₂ γ in these roles (21, 25). We excluded redox activation of iPLA₂ β , previously found in β -cell mitochondria (34).

In conclusion, our results elucidated iPLA₂ γ - plus UCP2-dependent regulation of mitochondrial superoxide production and insulin release in pancreatic β -cells. We describe a mechanism of free nascent FA-mediated antioxidant function, due to the synergic action of iPLA₂ γ and UCP2, counteracting mild sub-threshold lipotoxicity in pancreatic β -cells. The iPLA₂ γ -cleaved FAs may also participate in the lipid-mediated signaling such as in amplification of FA-induced insulin release *via* the GPR40 pathway.

The revealed redox activation of iPLA₂ γ and the requirement of nascent FAs for UCP2-mediated uncoupling ensure that the glucose sensing in pancreatic β -cells is not substantially affected by mild uncoupling, unless acute lipotoxicity and/or excessive oxidative stress activate the iPLA₂ γ /UCP2 antioxidant synergy. This synergy developed as an inherent antioxidant, cytoprotective, and specifically anti-lipotoxic mechanism that is protective before reaching a critical threshold and provides defense against long-term dysbalanced conditions, such as lipotoxicity. When these pro-oxidant impulses (stimulating otherwise antioxidant protection) are compromised, the inevitable self-accelerating vicious cycle leads to permanent oxidative stress, cell dysbalance, and the progression of type-2 diabetes pathology (15, 23). This progression has to be further elucidated and extended to future translational research.

Materials and Methods

Chemicals

r-BEL, s-BEL, and Trolox were purchased from Cayman (Ann Arbor, MI); MnTBAP was from Merck Millipore (Billerica, MA). All other reagents were from Sigma (St. Louis, MO).

Cell cultivation

Rat insulinoma INS-1E cells were a kind gift from Prof. Maechler, University of Geneva (37). Cells were cultivated with 11 mM glucose in RPMI 1640 medium with 2 mM L-glutamine, 10 mM HEPES, 2 g·l⁻¹ sodium bicarbonate, 1 mM sodium pyruvate, 5% (v/v) fetal calf serum, 50 μ M mercaptoethanol, 50 IU·ml⁻¹ penicillin, and 50 μ g·ml⁻¹ streptomycin (49). Cells were preincubated for 16 h in

cultivation medium containing 3 mM glucose. The desired final glucose concentration was adjusted just immediately before each measurement.

Cell transfections and silencing

A BLOCK-iT Pol II miR RNAi system (Life Technologies, Carlsbad, CA) has been employed to express miRNAs against UCP2. The two miRNA sequences, 5'-TACAGA GTCGTAGAGGCCAATGTTTTGGCCACTGACTGACAT TGGCCTACGACTCTGTA-3' and 5'-ATTTCCGGGCAAC ATTGGGAGAGTTTTGGCCACTGACTGACTCTCCCAA TTGCCCGAAAT-3', were designed using the BLOCK-iT RNAi Designer and annealed into double-strand oligonucleotides, which were inserted into the linearized miRNA expression vector pcDNA6.2-GW/EmGFP-miR. Individual miRNAs were chained up into tandem constructs. The vector with UCP2-miRNA or control miRNA plasmids was cloned by Gateway BP/LR reaction into pLenti6.2/V5-DEST expression vector, and final constructs were validated by DNA sequence analysis. Lentiviral expression plasmids were co-transfected with the ViraPower™ Packaging Mix (Life Technologies) into the 293LTV cells using Lipofectamine 2000 (Life Technologies). The lentiviral stock was used to transduce INS-1E cells, followed by selection of a stably transduced cell line by blasticidin and verification by a green fluorescent protein (GFP) inherent cytosolic reporter.

For catalase overexpression (17), pZeoSV2(+) vector bearing human catalase sequence (gift from C. Glorieux and Prof. J. Verrax, Université Catholique de Louvain, Belgium) was transiently transfected into INS-1E cells using Lipofectamine 2000 (2.5 ml·mg⁻¹ DNA).

To silence iPLA₂ γ or iPLA₂ β , pGFP-V-RS vectors (Origene, Rockville, MD) as specific expression cassettes were used with inserted 29-mer shRNAs, 5'-CAAACACTGGC ACTCTTCAAGCAACCATGTCAAGAGCATGGTTGCT TGAAGAGTGCCAGTGTGTTG-3' or 5'-CAGTAGTGTC CCAACTTGTCTCAAACCTCAAGAGGGTTTGAGAAC AAGTTGGTGACTACTG-3', respectively. The same vectors with inserted scrambled shRNA expression cassettes served as negative controls. INS-1E cells were transiently transfected using Lipofectamine 2000 (2.5 ml·mg⁻¹ DNA) and verified by the GFP cytosolic reporter. For GPR40 (FFAR1) or phospholipase PLD6 silencing, we used Silencer Select siRNAs (Life Technologies), cat. No. 4390771, IDs s141419 and s141420; or IDs s142381 and s142382. They were used in comparison *versus* negative control siRNA (cat. number 4390843). RNA oligonucleotides (20 + 20 pmol of siGPR40 *vs.* 40 pmol of negative control) were used.

High-resolution respirometry and fluorescent assays for $\Delta\Psi_m$ and ATP monitoring

Cells were trypsinized, counted by a Countess Automated Cell Counter (Life Technologies), and adjusted to 2×10^6 cells/ml. Respiration was detected by an Oxygraph 2k (cells at 37°C, isolated mitochondria at 30°C; Oroboros, Innsbruck, Austria). Rates taken 3 min after sequential additions of glucose, TBHP, or PA (when applied) were corrected for KCN-insensitive respiration. Five micromolars of tetramethylrhodamine ethyl ester (TMRE; Life Technologies) added immediately before the assay were used for $\Delta\Psi_m$ monitoring on an RF 5301 PC spectrofluorometer

(Shimadzu, Tokyo, Japan) in a stirred 2 ml cuvette with excitation at 561 nm (3 nm slit) and emission at 579 nm (5 nm slit). Trifluoromethoxy carbonyl cyanide phenylhydrazine (FCCP) was titrated to a maximum (respiration) or added twice ($\Delta\Psi_m$). ATP quantification was performed using ATP Assay bioluminescence kit HSII (Roche, Basel, Switzerland) and the spectrofluorometer at 557 nm (5 nm slit).

Confocal microscopy

A confocal inverted fluorescent microscope Leica TCS SP2 AOBS was employed, with a PL APO 100 \times /1.40–0.70 oil immersion objective (pinhole 1 Airy unit) and a sample chamber set to 37°C supplied with 5% CO₂. Cells were seeded on poly-L-lysine-coated 22 mm glass coverslips (Marienfeld, Lauda-Königshofen, Germany) at 0.25×10^6 cells/coverslip 2 days before the experiment or at 0.4×10^6 cells/coverslip 1 day before the transient transfection and 3 days before the experiment.

Confocal microscopy monitoring of cytosolic ROS and extracellular FAs

Cytosolic ROS monitoring was ensured by 10 μ M CellROX (Life Technologies) after 30 min loading, while excited at 633 nm with a 1.2 mW HeNe laser and collecting emission between 650 and 700 nm. An ADIFAB2 FA indicator (FFA Sciences, San Diego, CA) was used to monitor extracellular free FAs, while excited with a 405 nm diode laser and collecting emission between 430 and 645 nm.

Confocal microscopy monitoring of superoxide released into mitochondrial matrix

A triphenylphosphonium-conjugated dihydroethidine, MitoSOX Red (Life Technologies), was used to monitor rates (J_m) of *in situ* surplus superoxide release into the mitochondrial matrix (10). The surplus represents the portion of superoxide not neutralized by the matrix Mn-SOD. Using rates, any variations in initial background fluorescence are eliminated and the method is feasible for semiquantification of matrix-released superoxide even at low or collapsed $\Delta\Psi_m$ (10). Excitation was at 488 nm by a 20 mW Argon laser, with emission collected between 550 and 650 nm, while the GFP reporter was checked between 508 and 516 nm. Cells were loaded with 4 μ M MitoSOX for 15 min. A series of confocal images were taken every 30 s for 20 min (Supplementary Movie S1). Regions of interest corresponding to mitochondria were selected using the Ellipse software (ViDiTo, Košice, Slovakia). Changes of integrated fluorescence intensity were quantified from plots of fluorescence in the selected areas *versus* time.

Assay for insulin release

Cells were seeded at 0.4×10^6 cells/well in poly-L-lysine-coated 12-well plates 1 day before the transient transfection and 3 days before the experiment. Insulin release was assayed using Rat Insulin ELISA kit (U-E type; Shibayagi, Shibukawa, Japan) in Krebs-Ringer HEPES buffer containing 2 mM glutamine and 0.1% bovine serum albumin after 10 min of preincubation before glucose addition.

SDS-PAGE and Western blotting

Silencing was verified by SDS-PAGE followed by Western blotting on mitochondria isolated from cells and using primary antibodies against UCP2 (No. 662047; Merck Millipore) or in cell lysates for iPLA₂γ (PNPLA8 N-terminal, AP4706a; Abgent, San Diego, CA); otherwise, ATP-synthase β-subunit (ATPB, ab14730; Abcam, Cambridge, MA), TIM23 (611222; BD Biosciences, Franklin Lakes, NJ), β-actin (ab3280; Abcam), and horseradish peroxidase-conjugated goat anti-mouse or anti-rabbit secondary antibody, respectively (Sigma) were used. Blots were visualized using an LAS-1000 Imager, and quantitative image analysis was performed with ImageJ software.

iPLA₂γ reconstitution

The recombinant human iPLA₂γ was reconstituted into liposomes by adopting published protocols (20). The enzyme was purchased (PNPLA8; Novus Biologicals, Littleton, CO) or was cell expressed from a vector encoding His-tagged enzyme (GeneCopoeia, Rockville, MD) and affinity purified using a nickel resin column (Qiagen, Germantown, MD). Ten microgram per milliliter of Novus protein was dissolved in 1% *n*-lauroylsarcosine, passed through a Sephadex G-25-300 column, and equilibrated with an assay medium plus 0.1% *n*-octylpentaoxyethylene (Bachem, Bubendorf, Switzerland). One hundred microgram per milliliter of the affinity-purified protein had to be treated with 10 mM DTT and dialyzed against the assay medium, in order to reversibly modify the protein to its reduced form. A Sephadex G-25-300 column (0.5% *n*-octylpentaoxyethylene) was used to remove DTT. Aliquots in μg·(mg lipid)⁻¹ (0.04 Novus protein; 0.4–0.8 affinity-purified protein) were mixed with phospholipids (*Escherichia coli* total lipid extract supplemented with 20% bovine heart cardiolipin; Avanti Polar Lipids, Alabaster, AL), to yield 28% cardiolipin, 46% phosphatidylethanolamine, 12% phosphatidylglycerol plus 14% other lipid, and 1 mg·(mg lipid)⁻¹ *n*-octylpentaoxyethylene. Proteoliposomes were formed by detergent removal using Bio-Beads SM-2 (Bio-Rad, Hercules, CA). Both the intraliposomal and assay medium contained Na⁺ salts of TES (50 mM), SO₄²⁻ (80 mM), and EDTA (2 mM), pH 7.5. Sulfopropylquinolinium-based monitoring of FA release into the liposome interior or GC/MS analyses of cleaved FAs was performed.

Quantification of free FAs

Free FAs released in liposomes or cells were quantified using GC/MS (6890 gas chromatograph, 5973 mass spectrometer; Agilent Technologies, Palo Alto, CA). Reaction mixtures were extracted with acidic 2-propanol/*n*-heptane, treated with ether/diazomethane at room temperature for 20 min, and evaporated under argon. The methylated FAs were reconstituted in 100 μl of *n*-heptane and analyzed by GC/MS. FAs were identified/quantified in comparison with spectra of purified standards. FA total content in phospholipids was evaluated after hydrolysis by 0.5 M NaOH at 60°C for 30 min, and after acidification and extraction.

Acknowledgments

This project was supported by grants of the Grant Agency of the Czech Republic (P303/11/P320 to J.J.; 15-15-02051S

to M.J.; 13-02033 and 13-06666 to P.J.) and by the research project RVO67985823. The authors gratefully acknowledge the excellent technical assistance of Lenka Josková with cell cultivation, Jana Vaicová with immunoblotting and ELISA, and Jitka Smiková with plasmid isolations. The authors express their gratitude to Prof. Libor Vítek, M.D., Ph.D., from the First Faculty of Medicine, Charles University, Prague, for kindly providing them with GC/MS and to Prof. Vladimir Skulachev, from Moscow University, Russia, for providing them with SkQ1.

Author Disclosure Statement

No competing financial interests exist.

References

- Affouit C and Brand MD. Uncoupling protein-2 contributes significantly to high mitochondrial proton leak in INS-1E insulinoma cells and attenuates glucose-stimulated insulin secretion. *Biochem J* 409: 84–93, 2008.
- Affouit C, Jastroch M, and Brand MD. Uncoupling protein-2 attenuates glucose-stimulated insulin secretion in INS-1E insulinoma cells by lowering mitochondrial reactive oxygen species. *Free Radic Biol Med* 50: 609–616, 2011.
- Allister EM, Robson-Doucette CA, Prentice KJ, Hardy AB, Sultan S, Gaisano HY, Kong D, Gilon P, Herrera PL, Lowell BB, and Wheeler MB. UCP2 regulates the glucagon response to fasting and starvation. *Diabetes* 62: 1623–1633, 2013.
- Arsenijevic D, Onuma H, Pecqueur C, Raimbault S, Manning BS, Miroux B, Couplan E, Alves-Guerra MC, Gubern M, Surwit R, Bouillaud F, Richard D, Collins S, and Ricquier D. Disruption of the uncoupling protein 2 gene in mice reveals a role in immunity and reactive oxygen species production. *Nat Genet* 26: 435–439, 2000.
- Ashcroft FM and Rorsman P. Diabetes mellitus and the β cell: the last ten years. *Cell* 148: 1160–1171, 2012.
- Beck V, Jabůrek M, Demina T, Rupprecht A, Porter RK, Ježek P, and Pohl EE. High efficiency of polyunsaturated fatty acids in the activation of human uncoupling protein 1 and 2 reconstituted in planar lipid bilayers. *FASEB J* 21: 1137–1144, 2007.
- Berardi MJ, Shih WM, Harrison SC, and Chou JJ. Mitochondrial uncoupling protein 2 structure determined by NMR molecular fragment searching. *Nature* 24: 109–113, 2011.
- Carpinelli AR, Picinato MC, Stevanato E, Oliveira HR, and Curi R. Insulin secretion induced by palmitate—a process fully dependent on glucose concentration. *Diabetes Metab* 28: 37–44, 2002.
- Chan CB, De Leo D, Joseph JW, McQuaid TS, Ha XF, Xu F, Tsushima RG, Pennefather PS, Salapatek AM, and Wheeler MB. Increased uncoupling protein-2 levels in beta-cells are associated with impaired glucose-stimulated insulin secretion: mechanism of action. *Diabetes* 50: 1302–1310, 2001.
- Dlasková A, Hlavatá L, and Ježek P. Oxidative stress caused by blocking of mitochondrial Complex I H⁺ pumping as a link in aging/disease vicious cycle. *Int J Biochem Cell Biol* 40: 1792–1805, 2008.
- El-Azzouny M, Evans CR, Treutelaar MK, Kennedy RT, and Burant CF. Increased glucose metabolism and glycerolipid formation by fatty acids and GPR40 receptor

- signaling underlies the fatty acid potentiation of insulin secretion. *J Biol Chem* 289: 13575–13588, 2014.
12. Fedorenko A, Lishko PV, and Kirichok Y. Mechanism of fatty-acid-dependent UCP1 uncoupling in brown fat mitochondria. *Cell* 151: 400–413, 2012.
 13. Galetti S, Sarre A, Perreten H, Produit-Zengaffinen N, Muzzin P, and Assimacopoulos-Jeannet F. Fatty acids do not activate UCP2 in pancreatic beta cells: comparison with UCP1. *Pflugers Arch* 457: 931–940, 2009.
 14. Gao Q and Frohman MA. Roles for the lipid-signaling enzyme MitoPLD in mitochondrial dynamics, piRNA biogenesis, and spermatogenesis. *BMB Rep* 45: 7–13, 2012.
 15. Gehrmann W, Elsner M, and Lenze S. Role of metabolically generated reactive oxygen species for lipotoxicity in pancreatic β -cells. *Diabetes Obes Metab* 12: S2, 149–158, 2010.
 16. Giacca A, Xiao C, Oprescu AI, Carpentier AC, and Lewis GF. Lipid-induced pancreatic β -cell dysfunction: focus on *in vivo* studies. *Am J Physiol Endocrinol Metab* 300: E255–E262, 2011.
 17. Glorieux C, Dejeans N, Sid B, Beck R, Calderon PB, and Verrax J. Catalase overexpression in mammary cancer cells leads to a less aggressive phenotype and an altered response to chemotherapy. *Biochem Pharmacol* 82: 1384–1390, 2011.
 18. Goglia F and Skulachev VP. A function for novel uncoupling proteins: antioxidant defense of mitochondrial matrix by translocating fatty acid peroxides from the inner to the outer membrane leaflet. *FASEB J* 15: 1585–1591, 2003.
 19. Graciano MF, Valle MM, Kowluru A, Curi R, and Carpinelli AR. Regulation of insulin secretion and reactive oxygen species production by free fatty acids in pancreatic islets. *Islets* 3: 213–223, 2011.
 20. Jabůrek M, Miyamoto S, Di Mascio P, Garlid KD, and Ježek P. Hydroperoxy fatty acid cycling mediated by mitochondrial uncoupling protein UCP2. *J Biol Chem* 279: 53097–53102, 2004.
 21. Jabůrek M, Ježek J, Zelenka J, and Ježek P. Antioxidant activity by a synergy of redox-sensitive mitochondrial phospholipase A2 and uncoupling protein-2 in lung and spleen. *Int J Biochem Cell Biol* 45: 816–825, 2013.
 22. Jenkins CM, Han X, Mancuso DJ, and Gross RW. Identification of calcium-independent phospholipase A2 (iPLA2) beta, and not iPLA2gamma, as the mediator of arginine vasopressin-induced arachidonic acid release in A-10 smooth muscle cells. Enantioselective mechanism-based discrimination of mammalian iPLA2s. *J Biol Chem* 277: 32807–32814, 2002.
 23. Ježek P, Dlasková A, and Plecítá-Hlavatá L. Redox homeostasis in pancreatic β cells. *Oxid Med Cell Longev* 2012: 932838, 2012.
 24. Ježek P and Hlavatá L. Mitochondria in homeostasis of reactive oxygen species in cell, tissues, and organism. *Int J Biochem Cell Biol* 37: 2478–2503, 2005.
 25. Ježek J, Jabůrek M, Zelenka J, and Ježek P. Mitochondrial phospholipase A2 activated by reactive oxygen species in heart mitochondria induces mild uncoupling. *Physiol Res* 59: 737–747, 2010.
 26. Jitrapakdee S, Wutthisathapornchai A, Wallace JC, and MacDonald MJ. Regulation of insulin secretion: role of mitochondrial signalling. *Diabetologia* 53: 1019–1032, 2010.
 27. Klimova T and Chandel NS. Mitochondrial complex III regulates hypoxic activation of HIF. *Cell Death Differ* 15: 660–666, 2008.
 28. Krauss S, Zhang CY, Scorrano L, Dalgaard LT, St-Pierre J, Grey ST, and Lowell BB. Superoxide-mediated activation of uncoupling protein 2 causes pancreatic beta cell dysfunction. *J Clin Invest* 112: 1831–1842, 2003.
 29. Lee SC, Robson-Doucette CA, and Wheeler MB. Uncoupling protein 2 regulates reactive oxygen species formation in islets and influences susceptibility to diabetogenic action of streptozotocin. *J Endocrinol* 203: 33–43, 2009.
 30. Lei XG and Vatamaniuk MZ. Two tales of antioxidant enzymes on β cells and diabetes. *Antioxid Redox Signal* 14: 489–503, 2011.
 31. Leloup C, Casteilla L, Carrière A, Galinier A, Benani A, Carneiro L, and Pénicaud L. Balancing mitochondrial redox signaling: a key point in metabolic regulation. *Antioxid Redox Signal* 14: 519–530, 2011.
 32. Lin N, Chen H, Zhang H, Wan X, and Su Q. Mitochondrial reactive oxygen species (ROS) inhibition ameliorates palmitate-induced INS-1 beta cell death. *Endocrine* 42: 107–117, 2012.
 33. Lu H, Koshkin V, Allister EM, Gyulhandanyan AV, and Wheeler MB. Molecular and metabolic evidence for mitochondrial defects associated with beta-cell dysfunction in a mouse model of type 2 diabetes. *Diabetes* 59: 448–459, 2010.
 34. Ma Z, Zhang S, Turk J, and Ramanadham S. Stimulation of insulin secretion and associated nuclear accumulation of iPLA(2)beta in INS-1 insulinoma cells. *Am J Physiol Endocrinol Metab* 282: E820–E833, 2002.
 35. Mancuso DJ, Jenkins CM, Sims HF, Cohen JM, Yang J, and Gross RW. Complex transcriptional and translational regulation of iPLA2 γ resulting in multiple gene products containing dual competing sites for mitochondrial and peroxisomal localization. *Eur J Biochem* 271: 4709–4724, 2004.
 36. Mattiasson G, Shamloo M, Gido G, Mathi K, Tomasevic G, Yi S, Warden CH, Castilho RF, Melcher T, Gonzalez-Zulueta M, Nikolich K, and Wieloch T. Uncoupling protein-2 prevents neuronal death and diminishes brain dysfunction after stroke and brain trauma. *Nat Med* 9: 1062–1068, 2003.
 37. Merglen A, Theander S, Rubi B, Chaffard G, Wollheim CB, and Maechler P. Glucose sensitivity and metabolism-secretion coupling studied during two-year continuous culture in INS-1E insulinoma cells. *Endocrinology* 145: 667–678, 2004.
 38. Murakami M, Taketomi Y, Miki Y, Sato H, Hirabayashi T, and Yamamoto K. Recent progress in phospholipase A₂ research: from cells to animals to humans. *Prog Lipid Res* 50: 152–192, 2011.
 39. Negre-Salvayre A, Salvayre R, Augé N, Pamplona R, and Portero-Otín M. Hyperglycemia and glycation in diabetic complications. *Antioxid Redox Signal* 11: 3071–3109, 2009.
 40. Nishikawa T and Araki E. Impact of mitochondrial ROS production in the pathogenesis of diabetes mellitus and its complications. *Antioxid Redox Signal* 9: 343–353, 2007.
 41. Perevoshchikova IV, Quinlan CL, Orr AL, Gerencser AA, and Brand MD. Sites of superoxide and hydrogen peroxide production during fatty acid oxidation in rat skeletal muscle mitochondria. *Free Radic Biol Med* 61: 298–309, 2013.
 42. Pi J, Bai Y, Daniel KW, Liu D, Lyght O, Edelstein D, Brownlee M, Corkey BE, and Collins S. Persistent oxidative stress due to absence of uncoupling protein 2 associated with

- impaired pancreatic beta-cell function. *Endocrinology* 150: 3040–3048, 2009.
43. Prentki M, Joly E, El-Assaad W, and Rduit R. Malonyl-CoA signaling, lipid partitioning and glucolipotoxicity: role in beta-cell adaptation and failure in the etiology of diabetes. *Diabetes* 51: 405–413, 2002.
 44. Prentki M, Matschinsky FM, and Madiraju SR. Metabolic signaling in fuel-induced insulin secretion. *Cell Metab* 18: 162–185, 2013.
 45. Produit-Zengaffinen N, Davis-Lameloise N, Perreten H, Bécard D, Gjinovci A, Keller PA, Wollheim CB, Herrera P, Muzzin P, and Assimacopoulos-Jeannet F. Increasing uncoupling protein-2 in pancreatic beta cells does not alter glucose-induced insulin secretion but decreases production of reactive oxygen species. *Diabetologia* 50: 84–93, 2007.
 46. Quinlan CL, Goncalves RL, Hey-Mogensen M, Yadava N, Bunik VI, and Brand MD. The 2-oxoacid dehydrogenase complexes in mitochondria can produce superoxide/hydrogen peroxide at much higher rates than complex I. *J Biol Chem* 289: 8312–8325, 2014.
 47. Robertson R, Zhou H, Zhang T, and Harmon JS. Chronic oxidative stress as a mechanism for glucose toxicity of the beta cell in type 2 diabetes. *Cell Biochem Biophys* 48: 139–146, 2007.
 48. Robson-Doucette CA, Sultan S, Allister EM, Wikstrom JD, Koshkin V, Bhattacharjee A, Prentice KJ, Sereda SB, Shirihai OS, and Wheeler MB. Beta-cell uncoupling protein 2 regulates reactive oxygen species production, which influences both insulin and glucagon secretion. *Diabetes* 60: 27110–27119, 2011.
 49. Špaček T, Šantorová J, Zacharovová K, Berková Z, Hlavatá L, Saudek F, and Ježek P. Glucose stimulated-insulin secretion of insulinoma INS1-E cells is associated with elevation of both respiration and mitochondrial membrane potential. *Int J Biochem Cell Biol* 40: 1522–1535, 2008.
 50. St-Pierre J, Buckingham JA, Roebuck SJ, and Brand MD. Topology of superoxide production from different sites in the mitochondrial electron transport chain. *J Biol Chem* 277: 44784–44790, 2002.
 51. Szabadkai G and Duchon MR. Mitochondria mediated cell death in diabetes. *Apoptosis* 14: 1405–1423, 2009.
 52. Wang Y, Wang PY, and Takashi K. Chronic effects of different non-esterified fatty acids on pancreatic islets of rats. *Endocrine* 29: 169–173, 2006.
 53. Žáčková M, Škobisová E, Urbánková E, and Ježek P. Activating omega-6 polyunsaturated fatty acids and inhibitory purine nucleotides are high affinity ligands for novel mitochondrial uncoupling proteins UCP2 and UCP3. *J Biol Chem* 278: 20761–20769, 2003.
 54. Zhang CY, Baffy G, Perret P, Krauss S, Peroni O, Grujic D, Hagen T, Vidal-Puig AJ, Boss O, Kim YB, Zheng XX, Wheeler MB, Shulman GI, Chan CB, and Lowell BB. Uncoupling protein-2 negatively regulates insulin secretion

and is a major link between obesity beta-cell dysfunction and type 2 diabetes. *Cell* 105: 745–755, 2001.

Address correspondence to:

Dr. Petr Ježek

Department of Membrane Transport Biophysics, No.75

Institute of Physiology

Academy of Sciences of the Czech Republic

Vídeňská 1083

14220 Prague 4

Czech Republic

E-mail: jezek@biomed.cas.cz

Date of first submission to ARS Central, November 13, 2014; date of final revised submission, April 6, 2015; date of acceptance, April 15, 2015.

Abbreviations Used

BSA = bovine serum albumin
Ca _L = L-type Ca ²⁺ channel
DTT = dithiothreitol
FA = fatty acid
FASIS = fatty acid-stimulated insulin secretion
FCCP = trifluoromethoxy carbonylcyanide phenylhydrazone
GC/MS = gas chromatography/mass spectrometry
GFP = green fluorescent protein
GPR40 = G-protein-coupled receptor 40
GSIS = glucose-stimulated insulin secretion
IMM = inner mitochondrial membrane
K _{ATP} = ATP-sensitive K ⁺ channel
miRNA = microRNA
MnTBAP = Mn(III)tetrakis(4-benzoic acid)porphyrin
mtPLD = mitochondrial phospholipase D
ntg = nontargeting
OXPPOS = oxidative phosphorylation
PA = palmitic acid
PAPLA1 = phosphatidic acid preferring PLA1
PNPLAs = patatin-like phospholipase domain-containing lipases
R-BEL = R-bromo-enol lactone
Rcarn = acylcarnitine
RCoA = acyl-CoA
ROS = reactive oxygen species
RSIS = redox-stimulated insulin secretion
s-BEL = S-bromo-enol lactone
SOD = superoxide dismutase
TBHP = <i>tert</i> -butylhydroperoxide
TMRE = tetramethylrhodamine ethyl ester
UCP = uncoupling protein